JWST H2RG SCA Reset Anomaly and Random Telegraph Noise

Ori Fox[1], Bernard J. Rauscher[2], Robert J. Hill[3], Brent Mott[2], Augustyn Waczynski[4], Yiting Wen[5], Wei Xia-Serafino[4]

[1]University of Virginia*, [2]NASA's Goddard Space Flight Center, [3]SSAI Inc. , [4]Global Science and Technology Inc., [5]MEI Technologies

*This research was supported in part by NASA's Graduate Student Research Program (GSRP) fellowship award to U. Virginia

Fig.1 - The reset anomaly is characterized by a non-linear effect which appears in the early frames following pixel reset. Shown are 88 samples-up-the-ramp for a single pixel in the engineering grade SCA H2RG-S016. A linear fit (**$a + b*t_{int}$**) of the data (**red dash-dot**) can result in a systematic over-estimate of the dark current. The dark current can be estimated by a linear fit through later samples (**purple dash**), but this requires that some data be discarded. Furthermore, the linear regime of the ramp can vary between pixels. A better solution is to extract the linear component from of the reset anomaly using a best fit function. The best fit (**black solid**) indicates the anomaly can be approximated by an equation combining the linear component with an exponential component we believe to be attributed to RC charging effects in the hybrid (ROIC & detectors). The equation takes the form: $S = a + b*t_{int} + c * e^{t_{int}/d}$, where S is the integrated signal, t_{int} is the integration time, and a,b,c, and d are the four fitting parameters. The 4-parameter fit accurately represents over 70% of the non-linear pixels.

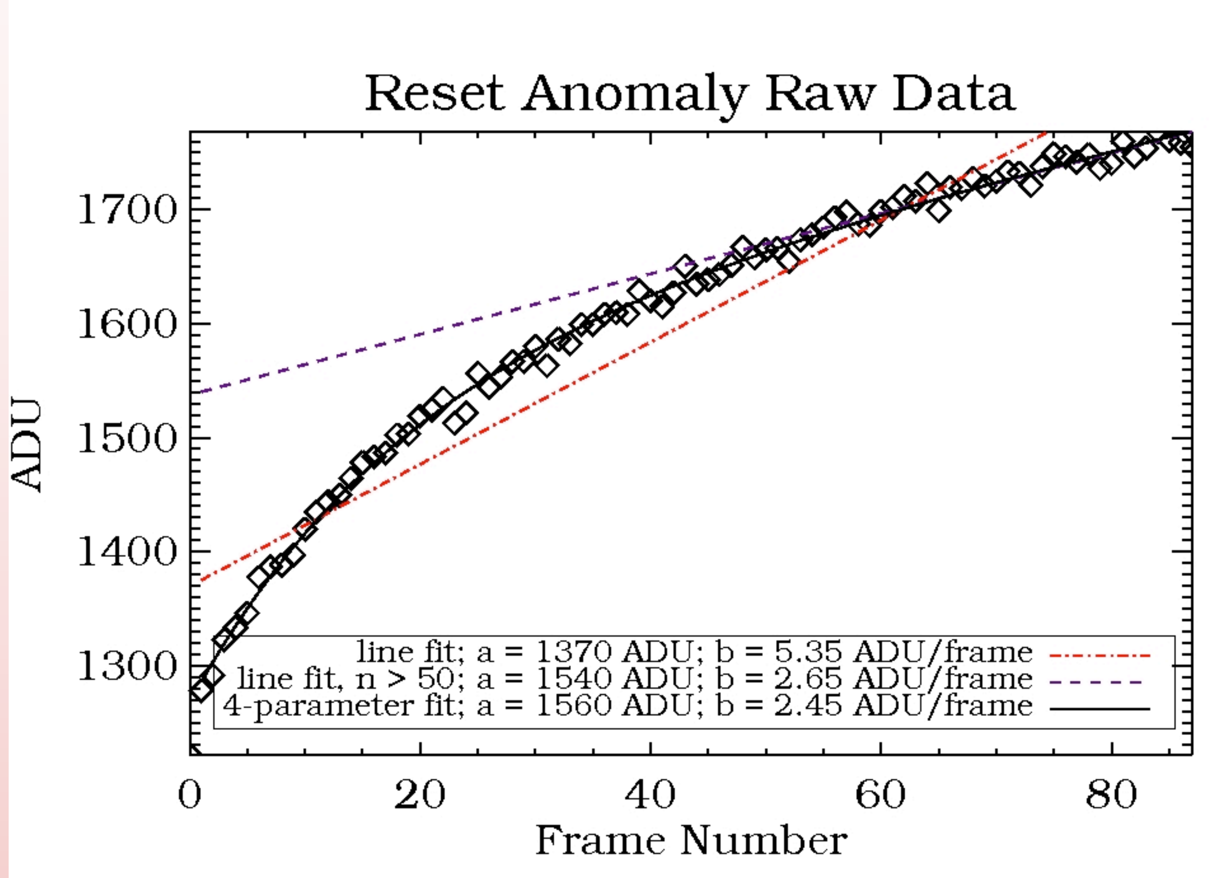

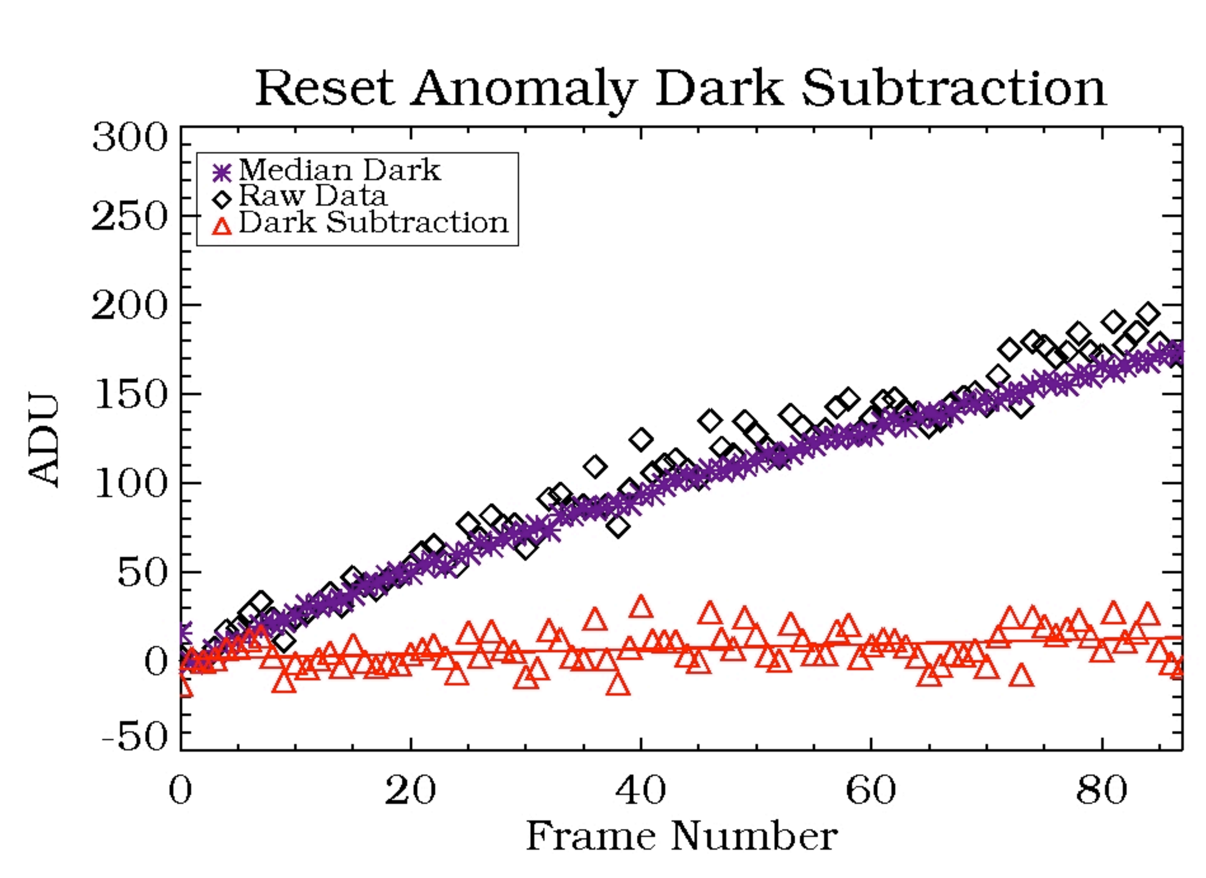

Fig.2 - The reset anomaly for a particular pixel (**black diamonds**) is a nearly noiseless instrument signature that can be removed by subtracting matching median dark cubes (**purple stars**) from each science integration. The subtraction (**red triangles**) is ideally a flat line with a y-intercept at y=0. In this figure, the unsubtracted data has been linearly shifted to match the y-scale of the subtracted data. The residual slope in the subtraction is attributed to the correlated noise from sample to sample and is indicative of shot noise and any correlated source of read noise on integrated dark current.

Fig.3 - A scatter is observed in the y-intercept offset (relative to 0) of the dark subtracted ramps. The histogram illustrates the distribution of offsets for 145 pixels in 99 exposures of the H2RG S016 SCA. The RMS is 31 ADU. This scatter is consistent with a combination of both KTC noise and inter-pixel capacitance. KTC noise is a result of a fluctuating potential on the capacitor at reset, given by the equation: $\sigma_{KTC}(e^-) = \sqrt{(KTC)}/e^-$, where k is Boltzmann's constant, T is temperature (in Kelvin), C is the capacitance, and e^- is the electron charge. Inter-pixel capacitance (IPC) consists of capacitive coupling that allows neighboring pixels to share charge and correlates the pixel outputs. It has recently been shown that IPC in SNAP HgCdTe detectors (which are similar to our arrays) can cause a 20% overestimate in the gain (Brown et al. 2006). Assuming IPC effects on gain to exist in the H2RGs at about the same level as in SNAP, the calculated KTC noise converted into ADU is consistent with the observed scatter in the SCAs.

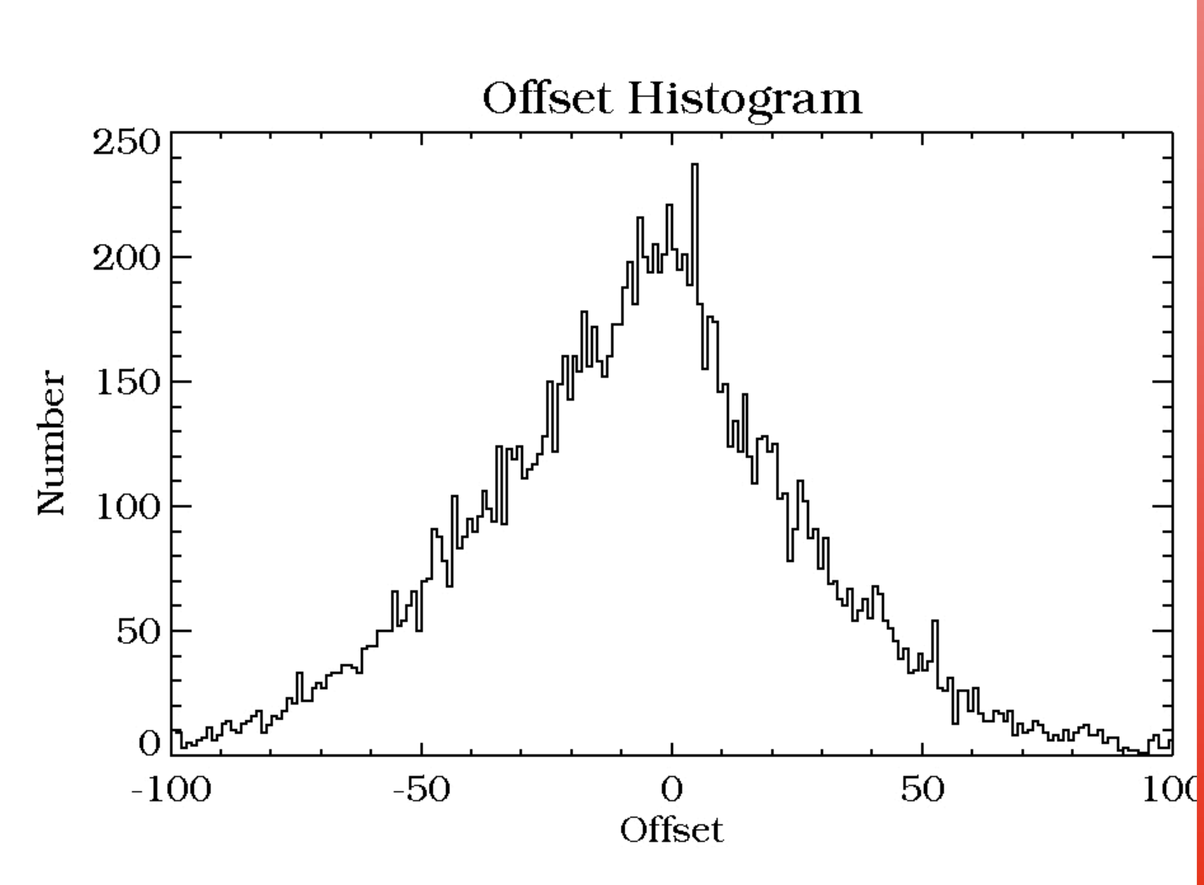

Fig.4 - Random Telegraph Noise (RTN) is characterized by a digital toggle between two (or more) levels. This figure illustrates the different patterns (Fig.4.a-d) RTN can exhibit. While the magnitude and frequency of the toggle varies between pixels, the noise is consistent for a given pixel from exposure to exposure. The source of the noise has been attributed to defects in the follower unit cell MOSFET in the Teledyne multiplexer (Bacon et al. 2005). The existence of a single defect can lead to trapped charge, which reduces the energy barrier between the two regions. As the charge is trapped or released, the current and thereby the output signal can change significantly.

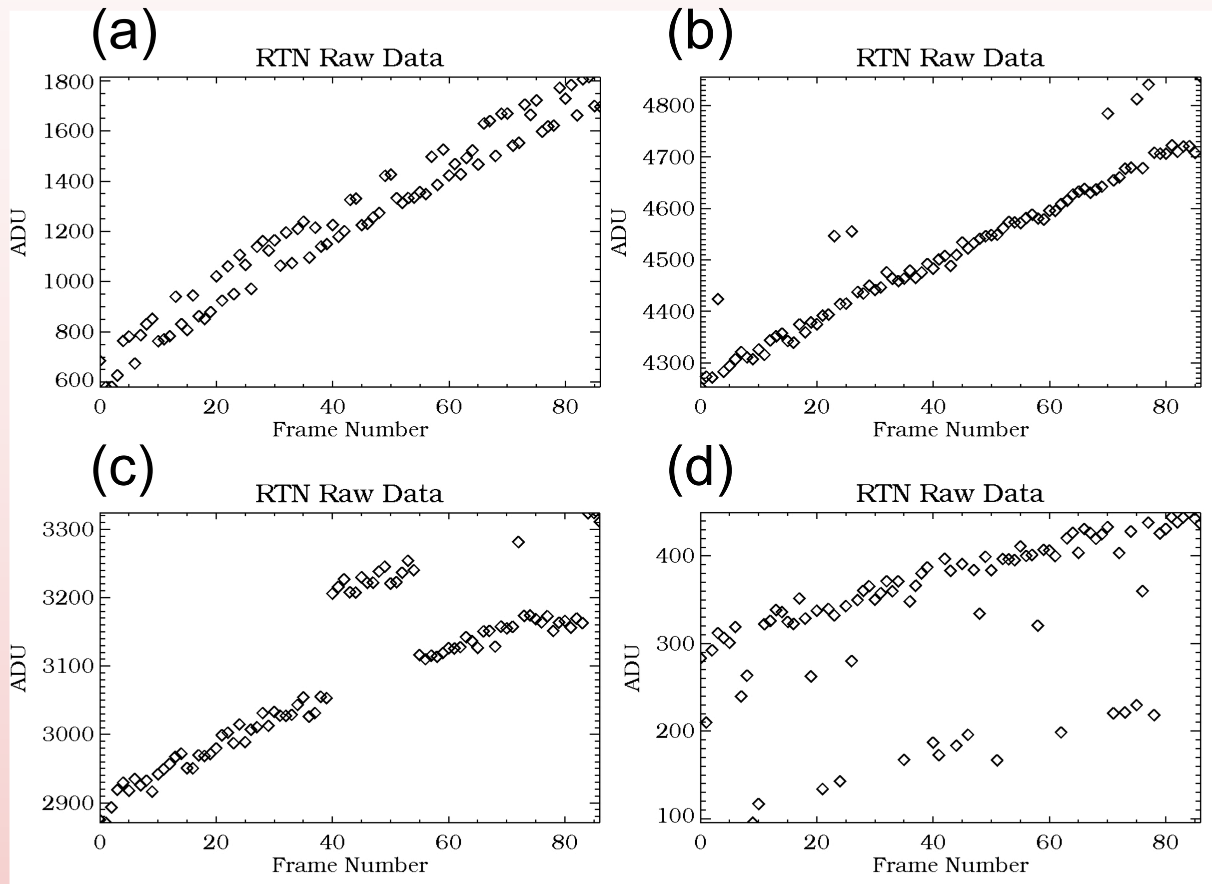

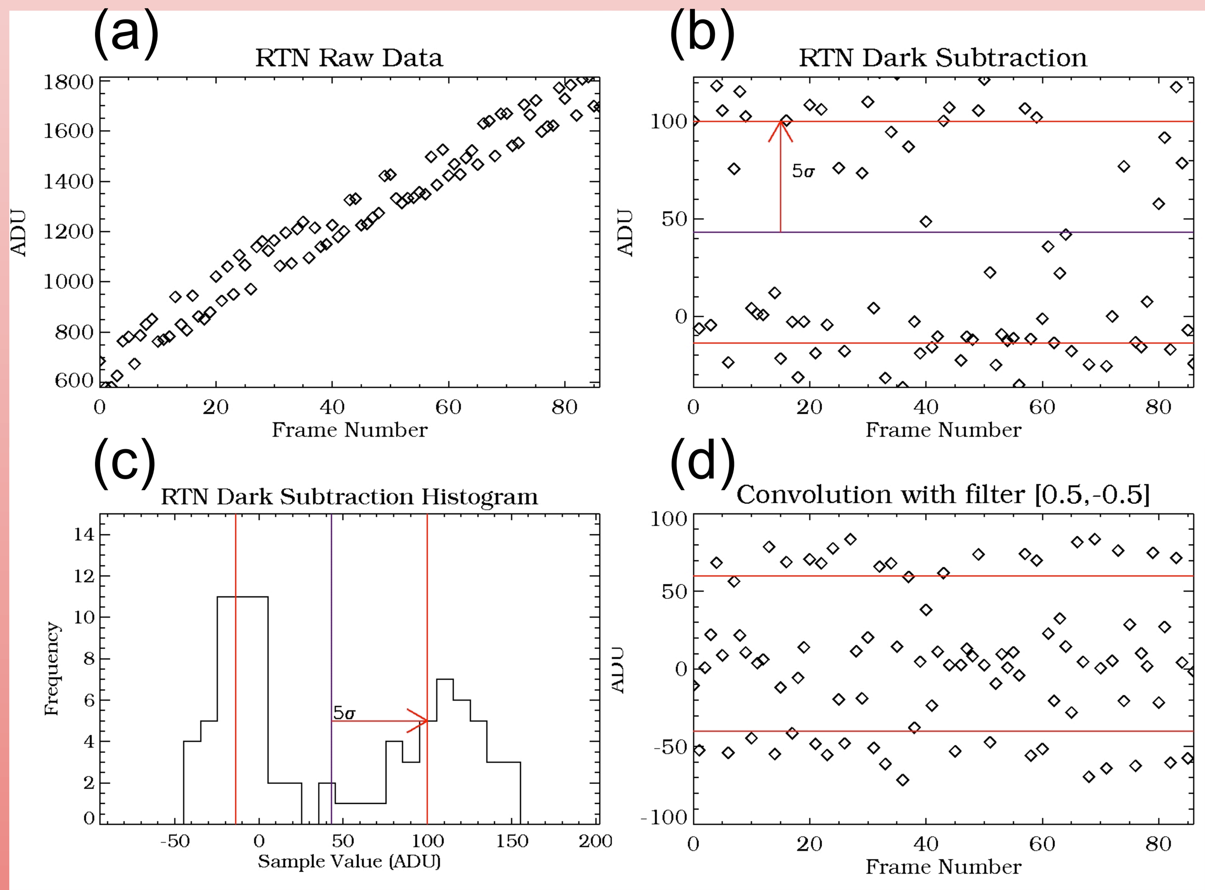

Fig.5 - We have developed an algorithm to detect RTN pixels in the H2RG-S016 SCA, such as the pixel shown in Fig.5.a. The algorithm consists of a two step process. First, we look for unusually noisy pixels with two unique populations. To remove dark current features, a median dark is subtracted from each exposure (Fig.5.b). A histogram of this data (Fig.5.c) illustrates the two populations indicative of pixels with RTN. For the average standard deviation of a subtracted ramp (σ), all pixels with data samples beyond 5*σ are flagged as possible RTN pixels. Second, a differential filter ([0.5,-0.5]) is convolved with the raw data of each flagged pixel (Fig.5.d). While typical pixels are expected to show a moderate rise (differential) between samples as the charge accumulates, RTN pixels have rapid rises and falls (>60 and <-40 ADU). These high detection thresholds are chosen to reduce the chance of a false detection because other noise sources rarely produce such large rises or falls. Of the RTN pixels detected, over 99% had real RTN features.

Fig.6 - RTN is observed to occur in only a fixed, small subset of pixels, making it a feature that is easily tracked with a pixel mask. For the H2RG-S016 SCA, 99 exposures were tested using the above algorithm. The histogram illustrates the consistency in which RTN was observed in a given pixel from exposure to exposure. The peak at bin 0 indicates that a vast majority of pixels (just under 100%) have no detectable RTN features in any of the exposures. The peak at bin 98 indicates that of pixels with a detectable RTN feature in one exposure, a majority have detectable RTN features in almost every other exposure. The noticeable peak at bin 1 and a drop off at bin 99 is because of the threshold limit in our algorithm. Inevitably, the RTN magnitude distribution statistics will sometimes push a pixel either below or above the detection threshold.